

BGA RE-BALLING FROM PB-FREE TO SN-PB METALLURGY

S. J. Meschter, S.A. McKeown, R. Feathers and E. Arseneau

BAE Systems

Johnson City, NY, USA

stephan.j.meschter@baesystems.com

ABSTRACT

As a result of a global movement away from using Lead (Pb) in electronic assemblies, component manufacturers are almost exclusively providing lead-free parts to satisfy the high volume consumer markets. Unfortunately, relatively little is known about the performance of lead-free solders in harsh vibration and shock environments. These concerns are amplified because the consumer industry is currently evaluating another generation of lead-free solder alloys in an effort to improve reliability. Tin whiskers not withstanding, nearly all the current lead-free electronic piece-part termination finishes are compatible with tin-lead assembly solder with the exception of ball grid arrays. Reprocessing lead-free BGAs with tin-lead ball metallurgy is one means of mitigating the risk of lead-free solder material failure modes such as tin whiskers, high cycle fatigue, printed circuit board pad cratering, and intermetallic fracture. In addition, because qualification of a metallurgy change in a high reliability application can take years, BGA reballing allows original equipment manufacturers to maintain the certification and qualification status on existing configurations while managing the on-going lead-free alloy changes occurring on BGAs. In the present work, an assessment of the mechanical integrity of four different commercially available BGAs was evaluated after reballing using visual inspection, cross-section evaluation, scanning acoustic microscopy, moiré interferometry, ball shear, ball pull and assembly level thermal cycling.

Key Words: Lead-free, Ball Grid Array, Solder, Reliability, Electronics, Reballing

Nomenclature and abbreviations:

BGA = Ball grid array
CTE = Coefficient of thermal expansion
CSAM = C-mode scanning acoustic microscope
Dia. = Diameter
Dims. = Dimensions
ENIG = Electroless nickel immersion gold
L = Length
 ΔL = Change in length of the specimen
Ni = Nickel
N_f = Number of fringes obtained
P = Phosphorous
Pb = Lead
PWB = Printed wiring board
SAM = Scanning acoustic microscope
SMD = Solder mask defined
Sn = Tin
T = Thickness

ΔT = Change in temperature, °C

T_g = Glass transition temperature

W = Width

BACKGROUND

Recent restriction of hazardous substances (RoHS) legislation from the European Union [1] as well as current environmentally friendly market trends [2] have resulted in the elimination of lead (Pb) from many electrical and electronic assemblies. Historically, electronic components have been manufactured using a tin-lead solder (typically, Sn63Pb37). The reliability of the tin-lead solders has been well documented and proven. The change from tin-lead to lead-free materials may be tolerable for many consumer electronic devices having a short life time and minor consequences of failure. However, lead-free use in long life high reliability systems having high consequences of failure that are used in the back bone of the defense, transportation, communication, and medical infrastructure needs to be fully understood.

The introduction of lead-free solder has brought on reliability concerns in high reliability applications having long service life and significant repair activity throughout the product's life cycle [3][4]. In addition to the tin whisker risks accompanying lead-free materials, designers are challenged by the higher processing temperatures, reduced vibration/shock performance and increased occurrences of brittle fractures of intermetallics and printed circuit board pads. Furthermore it may be undesirable to utilize lead-free bismuth-bearing solder alloys in high reliability repair depots because inadvertent mixing of tin-lead and bismuth bearing lead-free alloys can result in moderate to dramatic reductions in reliability [5][6].

High reliability designs have a long history of using mainstream consumer electronics and the DoD recognizes the advantages of dual use and commercial off the shelf (COTS) items. Sometimes it is possible to use the items directly, in other instances it is necessary to select parts based on certain performance parameters, and sometimes it is necessary to alter items in order to meet application requirements. In the present situation where lead-free ball grid arrays are unsuitable for use, it is possible to alter them by removing the lead-free balls and replacing them with tin-lead balls [7] [8]. For this investigation, when reballing suppliers were approached to reball from lead-free to tin-lead, several indicated that they already had considerable experience reballing tin-lead BGAs to lead-free during the early stages of the RoHS transition.

During the BGA reballing process, the lead-free balls are first removed, then the package is cleaned, the new tin-lead balls are attached and the package is cleaned again. One of the more challenging processes is ball removal because it tends to deviate from the standard surface mount reflow processes that BGAs are designed to withstand. Two common methods of ball removal are (1) solder wick and (2) flowing wave [7] [8]. The solder wick method has the advantage of lower overall package temperatures during processing than the flowing wave ball removal process. However, solder wick has the disadvantage of being a manual process that has locally higher heating at the individual solder pads. In addition, since solder wick braid comes in contact with the BGA during processing, there is increased risk of solder mask damage.

Once the balls have been removed, and the bottom side of the package has been visually inspected, the new tin-lead balls are then reattached. Ball reattachment also involves thermal processing of the part. Often a standard surface mount technology convection reflow process is used, but some reballing suppliers utilize laser soldering that typically results in low overall package heating. As long as the package integrity is maintained, the likelihood of electrical issues is low for most BGAs, especially since most are digital devices. In one study, extensive testing that included base loopback, top loopback, memory, flash, script and SRAM of devices after reballing showed no failures [8].

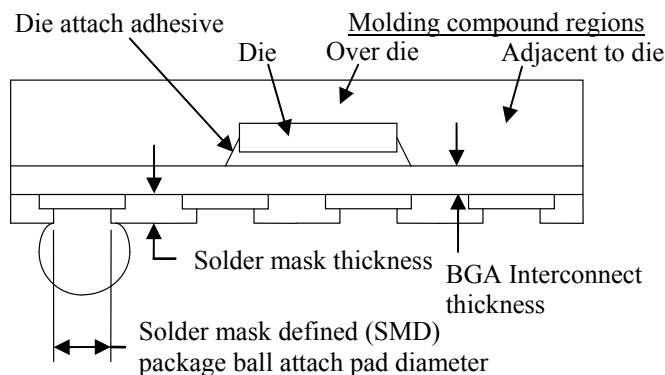


Fig. 1: BGA structure.

BGAs have relatively complex internal structures (Fig. 1) that can vary considerably from part to part. Since the reballing processing adds additional heat cycles to the BGA, the present work seeks to evaluate the mechanical integrity of the package after reballing.

In order to ensure a proper match between BGA type and reballing process an acceptance assessment is needed. Given the broad range of BGA constructions, it is likely that some BGAs will be tolerant to a broad range of reballing methods, while others will need more controlled process limits. An overall BGA reballing acceptance process flow is outlined in Fig. 2. Clearly, experience with a particular BGA manufacturer and construction type with a particular reballing process is a discriminator when formulating the BGA reballing assessment plan. BGAs with a nickel or an

electroless nickel (e.g. NiP) layer over the copper exhibit very little pad dissolution from the solder during reballing. Although use of gold over copper conductor under solder mask is not very prevalent, it does substantially increase the likelihood of solder mask separation which can result in solder tunneling under the solder mask [10]. The last part of the preliminary assessment in Fig. 2 is motivated by the fact that scanning acoustic microscopy (SAM) cannot be used to assess the internal integrity of some BGAs. Among the BGA features that inhibit acoustic microscopy are (1) packages with lids and cavities, (2) use of low modulus glob top layers over the die, (3) use of low acoustic density layers within the part and (4) complex BGA interconnect structures that attenuate acoustic energy. In the case where SAM cannot be used, other assessment methods must be employed.

When developing reballing acceptance requirements, it is important to avoid introducing requirements that exceed the original piece part requirements (e.g. warpage requirements after reballing cannot be more stringent than the requirements of the original part). An additional item that must be considered is that all manufacturing processes (e.g. dry baking, board soldering or environmental stress screening) result in some amount of change to the part. With that in mind, some part changes encountered during reballing may be acceptable and will not impact the reliability in the intended application.

EVALUATION METHODOLOGY

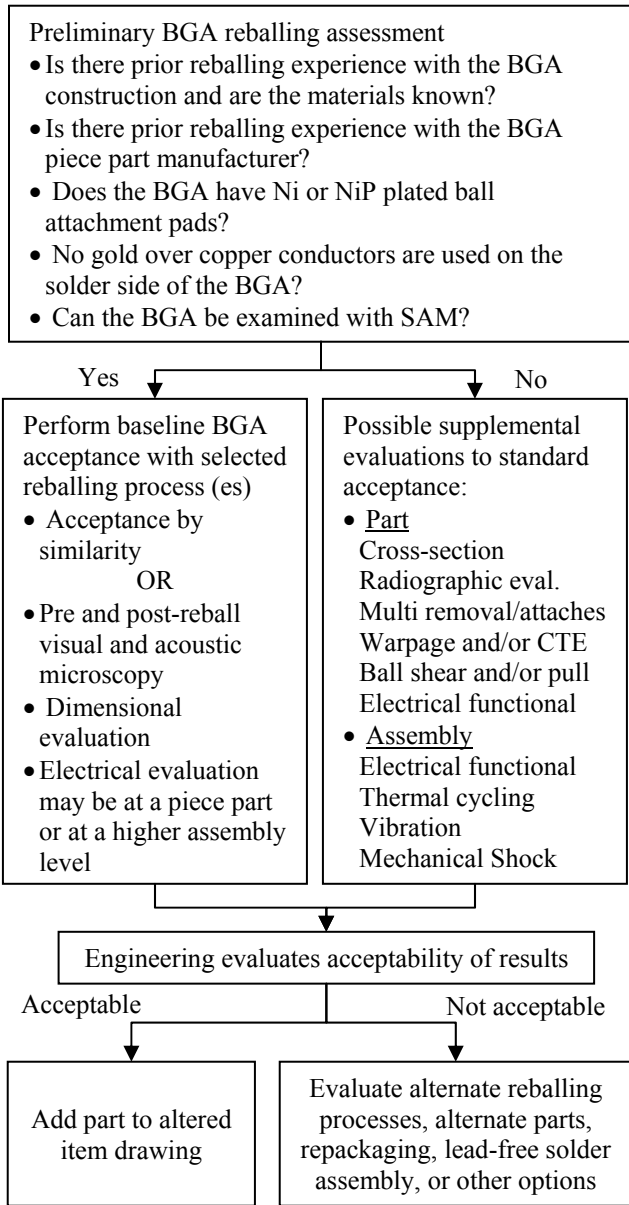
The BGAs under study are actual functional BGAs obtained from four different mainstream component manufacturers (designated M, L, F and X) so that real process variation from the supply chain would be included in the assessment. The sample type designation M90 indicates that the part is a 90 ball BGA from supplier M. These BGAs were selected to encompass a range of package sizes, die sizes, ball diameters and ball pitches as shown in Table 1 and Fig. 3. Three packages have wire bonded die (M90, L256 and F473) and one is a flip chip (X1148). Two of the BGAs were only available with lead-free balls. The L256 was available with either tin-lead or lead-free ball metallurgy allowing a unique comparison of various assessment parameters. The X1148 was only available with tin-lead ball metallurgy and was included to evaluate a tin-lead ball replacement/repair process.

The evaluations performed and the quantities of parts used in the present work are summarized in Table 2 and Fig. 4. The basic characteristics of the parts were obtained to facilitate modeling and future similarity analyses.

BGA Construction and Integrity Evaluation

Overall package measurements were made and compared with the datasheet. Photographs were obtained to record overall package details including the package marking. Cross-sectioning in conjunction with optical and scanning electron microscopy and radiographic imaging were used to determine the internal construction details needed for modeling and similarity analysis as shown in Fig. 1. The

cross-section also allowed an assessment of the internal molding compound and laminate integrity, the condition of the BGA interconnect board vias and traces, the internal die to package connections, as well as the solder mask adhesion to the BGA interconnect pads and surface copper features.



A detailed cross-section evaluation was also performed on the ball attach pads. The ball attach pad analysis included an optical or SEM image of a minimum of three BGA ball attach pads with balls removed showing diameter of BGA ball attach pad, thickness measurements of the copper and the nickel layers, a determination of the nickel type (electroless nickel, e.g. NiP alloy, or electrolytic nickel), and an assessment of the intermetallic. Since cross-sectioning is a destructive analysis, different BGAs were assessed before and after reballing. The cross-sectioning was complemented by radiographic imaging to determine the internal features of interest.

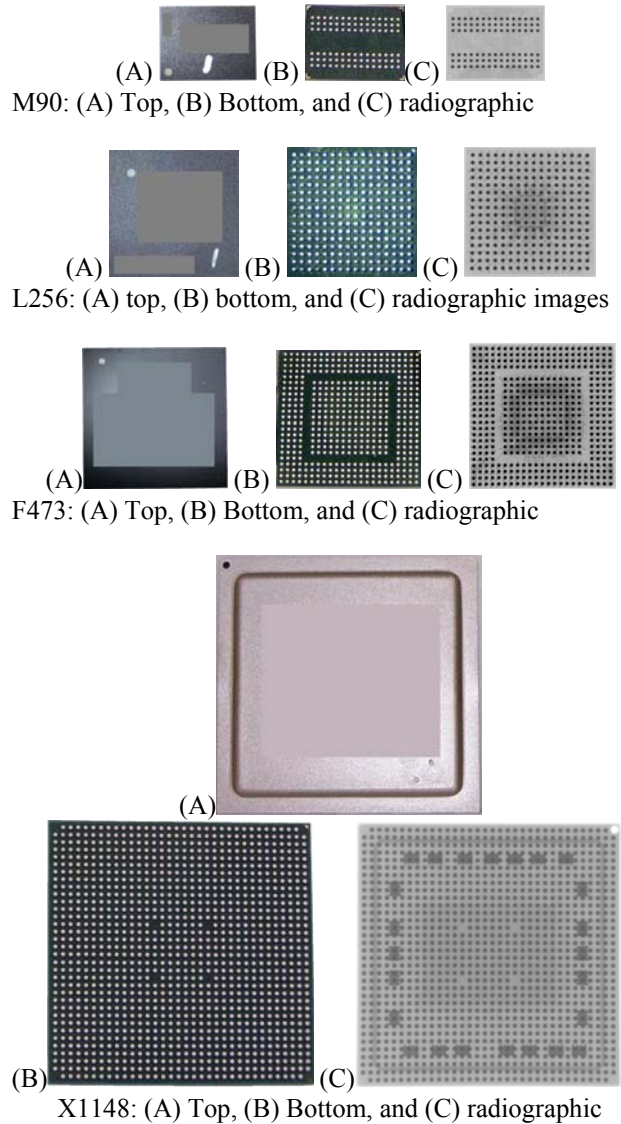


Fig. 2: Overall BGA reballing process flow

Table 1: BGA types and dimensions being evaluated (mm)

BGA	Pkg dims. (LxWxT)	Ball dia.	Ball pitch	Ball extents (LxW)	Die size
M90	13x10x0.65	0.45	0.8	11.2 x 6.4	7.53 x6.79
L256	17x17x1.25	0.5	1.0	15 x 15	4.28 x3.94
F473	19x19x1.12	0.4	0.8	17.6 x 17.6	6.23 x5.68
X1148	35x35x 2.8	0.6	1.0	33 x 33	19.3 x13.6

Fig. 3: Photomicrograph and radiographic images of the M90, L256, F473 and X1148 BGAs being evaluated.

Acoustic Microscopy and Visual Assessment Methods

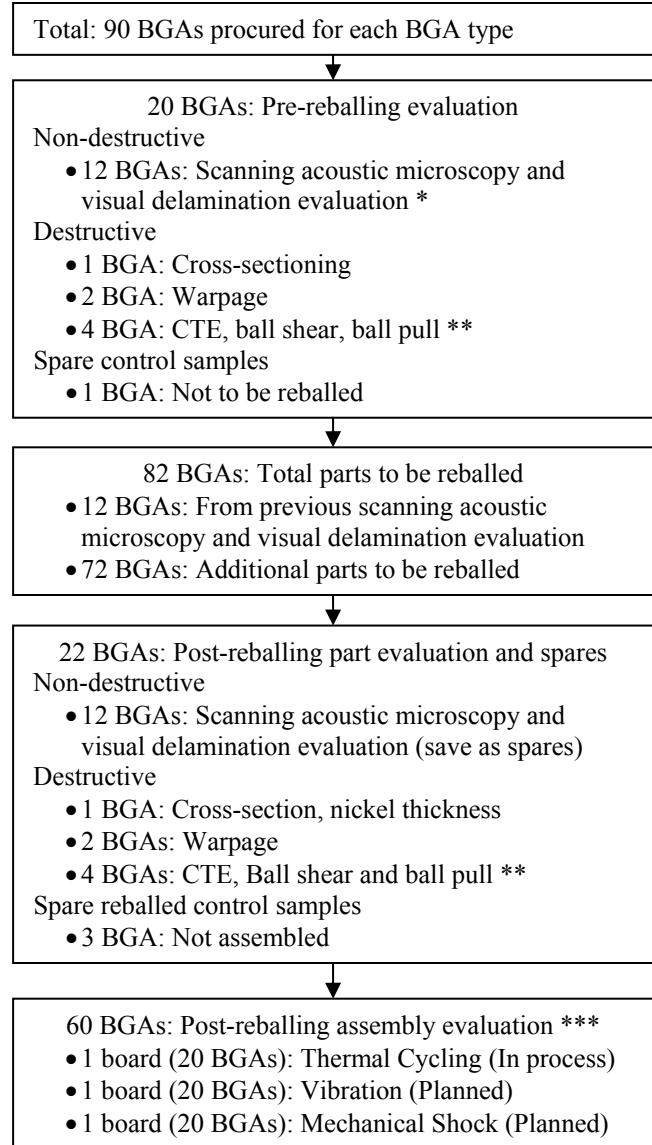
Scanning acoustic microscopy (SAM) and detailed visual inspections were performed on a sample of parts before and after reballing. SAM was performed to identify any delamination within the part at various critical intrapackage interfaces such as the die-top and molding compound, die

bottom and die attach adhesive, and the interconnect layer. SAM can also be useful for determining die size. Visual inspection was used to assess any surface breaking features. Often, combinations of C-mode reflected wave acoustic imaging (CSAM) and through scan acoustic microscopy can be used to evaluate the internal state of delamination in electronic parts. In the present work, equipment issues prevented using a through scan assessment and in one case cross-sectioning was needed to verify interface integrity. Scanning acoustic microscopy could not be used to assess the X1148 BGAs since acoustic waves could not traverse the void region under the lid.

Table 2: Parameters evaluated for each BGA type

Parameter	Description
One sample	
Overall photographs	Microphotographs of the top, side and bottom of the package being sure to capture all marking.
Radiographic examination	Determine die size and any significant metal structures.
BGA ball diameter	Assessment of BGA ball diameter uniformity by reballing supplier.
Cross-section of the package	Obtain internal construction details needed for modeling and similarity analysis.
Cross-section of BGA ball attach pad	Cross-section assessment of a typical ball attach pad before and after reballing.
BGA Pad metallization	Measure amount of BGA pad metal dissolution due to re-balling.
Pad intermetallic(s)	Evaluate intermetallic voiding, cracking, morphology evaluation
Package CTE	Performed using cross-sectional Moiré interferometry
Package warpage	Shadow Moiré interferometry measurements giving package warpage over the use and soldering temperatures.
Ball shear before and after reballing	High speed ball shear testing was performed according to JEDEC JESD22-B117A at a velocity of 1m/s.
Ball pull before and after reballing	High speed pull testing was performed according to JEDEC JESD22-B115 at a velocity of 100 mm/s.
Ten samples	
Scanning acoustic microscopy	C-Mode and through scan acoustic microscopy for delamination evaluation
Visual inspection	40x optical inspection for external cracks.
All parts	
Visual inspection	In accordance with J-STD-001, any visual damage in excess of part specification is cause for rejection.
Verification of ball diameter	Ball diameter measured for compliance with original manufacturer's requirements

Furthermore, since reflected sound waves are generated each time a different acoustic density is encountered in the interconnect area, reflections are generated from the copper traces, copper plane layers, vias, glass fibers, and solder mask layers making it difficult to resolve delaminated regions.



Notes:

* A minimum of ten BGAs are needed for acceptance testing. Some additional parts were included in case anomalies in as-received parts would prevent evaluation.

** ½ of the part is needed for CTE so ½ can be used for ball shear and/or ball pull

*** 20 BGAs are needed for each test board assembly. Each board has 12 functionally monitored BGAs and four BGAs for cross-sectioning with four reworked BGAs (removed and replaced).

Fig. 4: Reballing BGA part utilization for each BGA type.

The C-mode scanning transducer head frequency was selected in accordance with IPC/JEDEC J-STD-035 paragraph 4.1.1 to obtain maximum image resolution at the regions of interest. A transducer ranging in frequency from 15 to 50 MHz was used, with corresponding spot sizes from 0.180 to 0.073 mm. The coupling medium used in the containment tank was distilled water.

The amount of delamination detected over each area of interest was totaled by an automated process before and after reballing. A minimum of ten parts were individually serialized and evaluated for cracking/delamination before and after reballing. Parts exhibiting anomalies preventing measurements before re-balling are allowed to be replaced, but this was not necessary in the present evaluation.

Delamination measurements were compared before and after reballing. A delamination area (or length) change was defined as a percentage change computed from the delaminated area (or length) divided by the total area (or length) of interest. The following thresholds were used for acceptance:

- Any external crack visible using a 40X optical microscope was evaluated to ensure that it did not increase by more than 10%.
- Any internal cracks that intersected a bond wire, ball bond or wedge bond were evaluated to ensure that they did not increase by more than 10%.
- Any internal cracks extending from any internal feature to the outside of the package were evaluated to ensure that they did not increase by more than 10%.
- No delamination on the active side of the die was permitted.
- If applicable, no delamination change > 10% on any wire bonding surface of the die paddle (down bond area) or the lead frame of LOC (lead on chip) devices.
- If applicable, no delamination change > 10% along any polymeric film bridging any metallic features that are designed to be isolated (verifiable by through transmission acoustic microscopy and/or CSAM imaging from the opposite side as required).

For example, if the total die paddle area was 0.100 square inches (62.5 square mm) and had a pre-existing delamination of 3 percent (0.003 square inches or 1.88 square mm) before reballing, the delamination would be allowed to increase to a value less than 13 percent of the area of interest (0.013 square inches or 8.39 square mm) after reballing.

Warpage Measurement Method

Component warpage was measured according to JEDEC JESD22-B112 and JEITA ED-7306 standards. An Akrometrix TherMoiré PS200 system was employed, using a 100 line per inch grating. This grating provides a measurement resolution of at least 2.54 microns (0.1 mils), of out-of-plane displacement.

Two of each BGA type were prepared by mechanically removing the solder balls using a shear tool. The ball-attach side of each sample was then lightly dusted with a coat of high temperature white paint to gain the necessary contrast for the measurement technique. All warpage measurements were made on the ball-attach side of the components. The measurements were taken with the solder ball side facing up. The thermal profile used to test each sample is shown in Fig. 5. A peak temperature of 245 °C was selected, and measurements were made at the temperatures indicated by the circles in the profile figure. Of particular interest were the warpages near the maximum service temperatures (100 and 125 °C), the warpage near the tin-lead eutectic melting temperature (175 and 183 °C) where head-in-pillow defects could occur, the warpage at the maximum tin-lead solder profile (220 °C) and the maximum lead-free solder profile (245 °C).

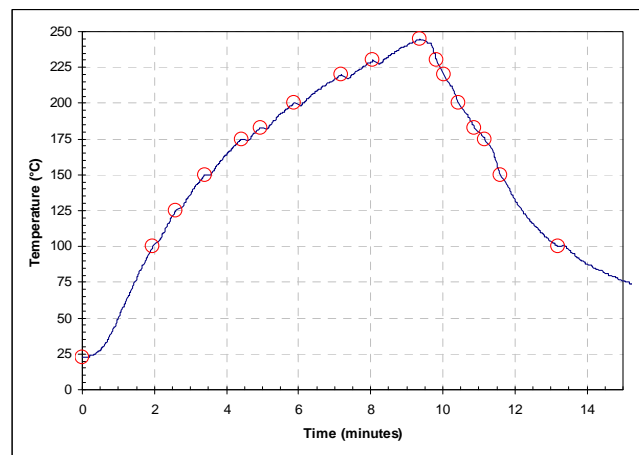


Fig. 5: Heating profile use for the warpage measurements (red circles indicate temperatures where warpage data was obtained)

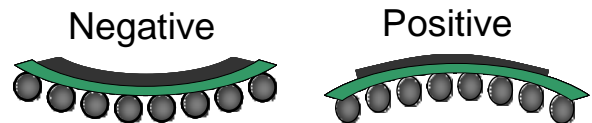


Fig. 6: Definition for positive and negative warpage directions

Since warpage was measured through the heating and the cooling ramps, it was possible to verify that the BGA under test returned to its original warpage state after exposure to the peak reflow temperature.

The total component warpage was defined per JEITA ED-7306, in which the measurement zone included only the solder ball attachment area. Plots of warpage versus temperature were generated by averaging the data across each diagonal. Positive warpage was defined as the condition where the center of the component was lifted from the seating plane, while negative warpage was defined as the condition where the corners of the component were lifted, as indicated in Fig. 6.

Coefficient of Thermal Expansion Measurement Method

All materials have a tendency to change in length in response to a change in temperature. This material property is called the material's coefficient of thermal expansion (CTE). Coefficients of thermal expansion for electronic packaging materials can range from 4-ppm/°C for the silicon die, to 17-ppm/°C for glass epoxy PWB material, to 28.3-ppm/°C for tin-lead solder. The average CTE of a BGA package varies with the materials and geometries used in its construction. As with warpage, a change in the BGA material properties or internal delamination from the reballing process might be revealed in differences in CTE.

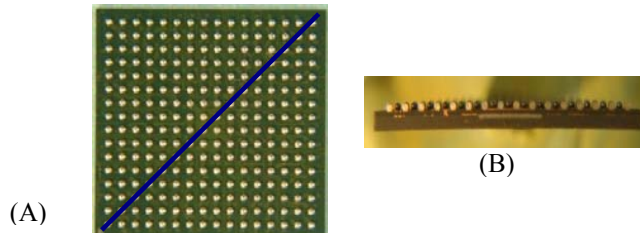


Fig. 7: Typical section where plane along which the CTE is measured. (L256 shown).

In the current evaluation, Moiré interferometry [11] was used to measure the BGA CTEs at Binghamton University. Moiré interferometry is an optical method, providing wholefield contour maps of in-plane displacements. In this method, a high frequency crossed-line diffraction grating is replicated on the surface of the specimen and it deforms together with the underlying specimen. Coherent beams from a laser are used to create a virtual reference grating. The deformed specimen grating and reference grating interact to produce the Moiré fringe pattern with each fringe corresponding to the magnitude of movement between the BGA and the reference grid.

In the present evaluation, the CTE was measured on four BGA samples, two in an as-received condition and two that had been reballed. To measure the CTE of the BGAs, the BGAs were cut along their diagonal as shown in Fig. 7. Then a polymer grating was bonded to the BGA at a temperature of 80 °C. Both the BGA and the grating contract upon cooling to room temperature and when the virtual laser reference grid is projected onto the grating, Moiré fringes are formed. For the present system sensitivity, each fringe represents a displacement of 0.417 microns and the CTE can be determined from the following computation:

$$\text{CTE} = \text{Coefficient of thermal expansion} = (\Delta L/L) \cdot (1/\Delta T)$$

L = Length of the BGA over the region of interest.

ΔL = Change in length of the specimen

with $\Delta L = N_f \cdot \text{Sensitivity of the equipment, which is 0.417 micron displacement per fringe}$

N_f = Number of fringes

ΔT = Change in temperature, °C

For example $\Delta T = 59.3$ °C is the temperature difference obtained when the replication temperature is 80°C and room temperature is 20.7 °C.

Shear and Ball Pull Test Method

Solder ball pull and shear testing gives an indication of the interconnect strength and failure mode in the ball attach pad region under various rates of loading. For this testing, comparisons were made between the as-received BGA devices and those that were reballed. Shear testing was performed according to JEDEC JESD22-B117A, while pull testing was performed according to JEDEC JESD22-B115. The failure force, energy and failure mode were recorded for each trial and tabulated for each component.

Testing speeds were selected based on the desired failure mode. The goal of this testing was to determine the robustness of the solder ball interface with the BGA attachment pad and observe any changes due to the reballing process. A test speed of 1-m/s was selected for shear test, and 100-mm/s for pull test. These test speeds were selected because they were expected to produce interfacial failures on lead-free solder joints based on previous testing experience. Two BGAs of each type were selected for pull testing, and two additional BGAs were selected for shear testing. Pull testing was performed on 16 solder balls per component, or 32 solder balls per component type.

Sample preparation for shear testing required that the component be depopulated of solder balls except for a single outer row to be tested. For this reason, as well as component clamping requirements, only 9 solder balls per M90 BGA and 12 solder balls per L256 BGA could be tested in shear.

BGA Analytical Modeling Method

Finite-element analysis (FEA) was used to determine the internal stresses resulting from reballing. The analytical effort concentrated on the ball removal process. During ball removal with liquid solder contacting the bottom of the BGA, the thermal conditions are considerably different than with the surface mount convection reflow typically used for soldering. In the present work, an overall warpage model that could be correlated to the warpage testing was created for the L256 and the F473 BGAs. In addition, the maximum L256 BGA package stresses during ball removal were determined for two different ball removal thermal profiles. One profile was based on the measured package temperatures during ball removal in the present work, and the other had a higher preheat and higher wave solder temperature that might occur in a modified process. The maximum ball removal stresses were compared to the maximum standard surface mount reflow stress.

First a finite-element half-symmetry model was developed (see Fig. 8) and a transient thermal analysis was used to determine the temperature distribution inside the part. The computed thermal response was compared to the measured temperatures at the front of the package, the top center of the die and the rear of the package during ball removal.

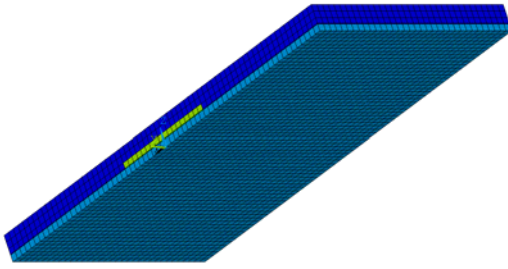


Fig. 8: BGA Finite-Element Model

When the thermal FEA was completed, the thermal elements were converted to structural elements and a static structural analysis was conducted to calculate internal stresses. The parametric modeling capabilities of the ANSYS finite-element code was used to automatically generate the model based on datasheet and measured part dimensions. The L256 BGA model has 54,921 nodes and 11,560 hexahedron (20-node) elements while the F473 BGA model is larger with 97,008 nodes and 21,294 hexahedron (20-node) elements.

Material properties for most inorganic electronic packaging materials (excluding solders) are well defined and not subject to large variations over typical electronic packaging temperature ranges, because typical service operation is at relatively low homologous temperatures. This assertion is not valid for polymer materials when the glass transition temperature (T_g) is exceeded. Thermal expansion data is frequently used to determine the T_g , so thermal expansion values above and below it are readily available as published material properties. However, the elastic modulus is also reduced above T_g , and it is important that models also include this effect. This relationship is especially significant for die bond materials, which usually have T_g values much lower than typical molding compounds. Since soldering process temperatures routinely exceed typical T_g values, modeling of electronic package stresses during soldering requires that both thermal coefficient of expansion and modulus changes above the T_g be included. Details on the temperature-dependent material modeling approach used here can be found in Reference [13]. The specific material properties used in the present work were calibrated so that the steady-state thermal analysis matched the measured warpage and CTE values obtained during the testing. Following calibration, the transient thermomechanical analysis was performed that simulated the BGA package bottom moving over the flowing solder wave.

Thermal Cycling Test Method

The reballed BGAs were soldered onto custom designed circuit boards to evaluate assembly level thermal cycling reliability. A typical test module assembly is shown in Fig. 9. The input/output connectors, interface circuitry and prognostics health monitoring circuitry are on the left side of the card. There are 12 electrically monitored BGAs in the center and the four BGAs for cross-sectioning are located on the right break-off portion of the assembly. The modules are individually serialized and marked with the year and month

that the assembly was soldered. The prognostics circuitry stores temperature data during the thermal cycling. The boards utilize boundary scan circuitry and/or custom circuits to monitor the continuity of select BGA balls during thermal cycling. The assembled boards were placed in a thermal cycling chamber and the chamber ambient was cycled from -55 to +95 °C with half hour ramps and dwells. Since the modules were widely spaced and exposed directly to the circulating chamber air, their temperature had no more than a ten minute lag from the chamber temperature during the transitions.

BGA REBALLING PROCESS

Reballing was performed using soldering methods in accordance with J-STD-001 Class 3. The balls were removed using a flowing solder wave methodology with the devices preheated to a range of 120 to 160 °C before contacting the tin-lead eutectic solder wave. The liquid solder wave was maintained at 230 °C. A typical ball removal thermal profile is shown in Fig. 10. The process begins by placing the part in a fixture with the ball side facing downward toward the wave. The fixture is then placed on the moving machine fingers at a velocity of 80-cm/minute, moving through a preheating stage, the flowing solder wave, and finally to a supplier proprietary pad leveling process.

The part is in contact with the flowing solder wave for approximately 5 seconds. The thick lines in Fig. 10 show the computed finite element model thermal responses of the package (front, die top center and rear) and the thin lines represent the measured data. Note that the BGAs cooled as it traversed the short distance between the preheater and the solder wave, and again between the solder wave and the pad leveling process. Throughout the reballing process, the BGAs were treated as moisture sensitive devices in accordance with J-STD-033. (Note: The CSAM evaluation parts were baked dry prior to reballing.)

After ball removal, the packages were cleaned to remove ball removal flux and inspected. The ball attach proceeds next. Flux was applied to the package, Sn63Pb37 balls were placed on the pads, the package was reflowed in a standard surface mount convection reflow oven (peak part temperature = 225 °C), cleaned, and then inspected. The solder ball composition was in accordance with J-STD-006, Table A-2. The flux was a low activity flux (ORLO per J-STD-004).

After the alteration, the ball geometry was verified to insure that it met the dimensional requirements of the original part drawing, and inspected for any defects that would degrade the operation or reliability. Component cleanliness was verified through ionic cleanliness testing and visual inspection. After reballing, the parts were marked with a yellow dot to allow differentiation from non-reballed parts and serialized to facilitate tracking through testing.

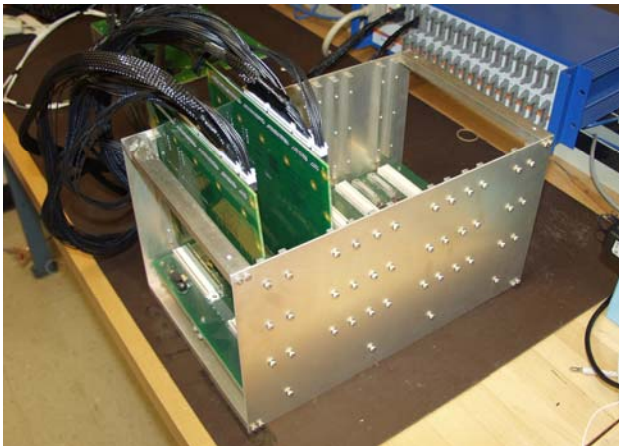
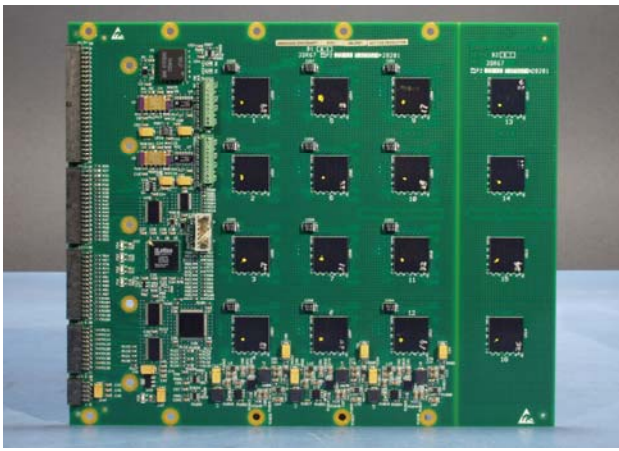


Fig. 9: Photograph of a typical thermal cycling test board (top), board chassis used in thermal chamber (middle) and test equipment (bottom).

RESULTS AND DISCUSSION

In-process Inspection

All the packages passed the ball size dimensional inspection. In addition, the BGAs were visually inspected after ball removal and again after ball re-attachment. Out of the 360 BGAs processed in the present activity, only two parts were rejected. One BGA had a missing pad and a cracked pad (See Fig. 11) and one exhibited bottom side delamination (Fig. 12).

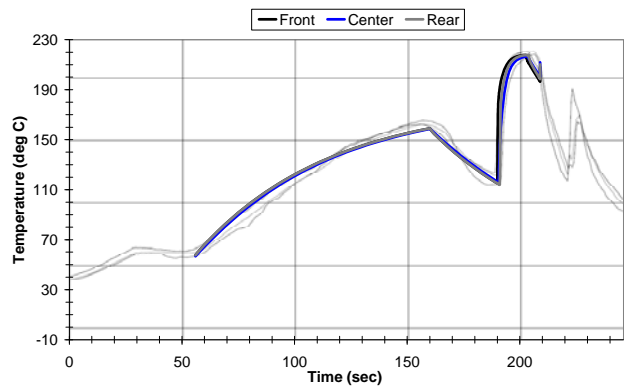


Fig. 10: Typical BGA ball removal thermal profiles (L256 shown). Fine lines are measured data and bold lines are the model results. The package front, the die top center and the package rear temperatures were measured and modeled.

Physical Measurements of BGA Features

The results of the overall measurements indicate that the physical BGA package dimensions were not impacted to any significant degree by the reballing process. The cross-section and radiographic inspections did not reveal any detectable changes or damage to the BGA packages with respect to internal layers, bump configuration, inner layer traces, wire bonding, die attachment, or passive components where present.

A typical cross-section of the overall package is shown in Fig. 13. In general, all BGA interconnects were constructed of copper base foils with electroless nickel (e.g. NiP alloy) / immersion gold (ENIG) finish on bump attach pads. All pads were solder mask defined (SMD), with ENIG processing occurring after the application of solder mask. Intermetallic formations seen on the reballed BGAs all appear to be robust with no indications of voiding, separation, excess oxidation, porosity, or lack of solderability.

No internal damage was identified during the sectioning that was not externally visible during the in-process inspection. Cross-sections of the internal BGA interconnect circuit boards were found to be acceptable to IPC-6012B and IPC-A-600 for both the as-received and reballed BGAs. Sections were reviewed in both un-etched and chemically etched preparations. Cross-sections were reviewed for solder mask coverage and registration, surface and inner layer copper integrity, ENIG finish homogeneity, laminate integrity, and plating process. No issues were detected in either the as received or reballed packages. A summary of the measurements obtained from the cross-sections are given in Table 3. The BGA ball attach pad and solder ball metallurgy details of both the original lead-free ball and the reballed tin-lead ball are shown in Fig. 14.

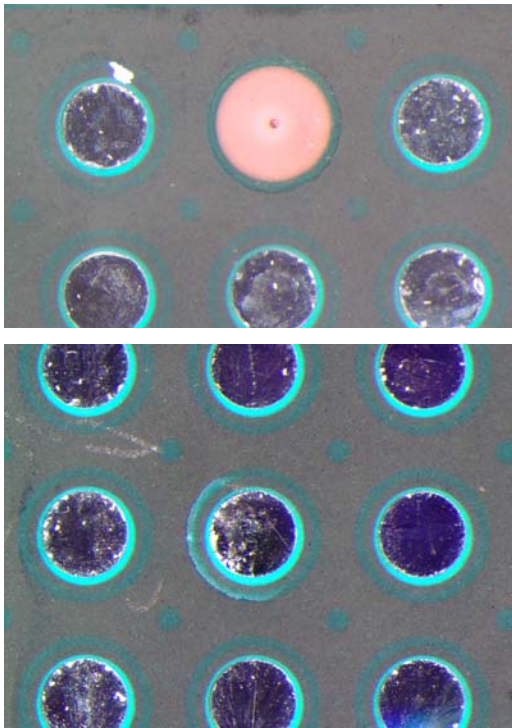


Fig. 11: Photomicrograph BGA X1148 SN1 package bottom after ball removal showing a missing pad (top) in one location and fracture around a pad in another location (bottom). Anomalies were found after ball removal.

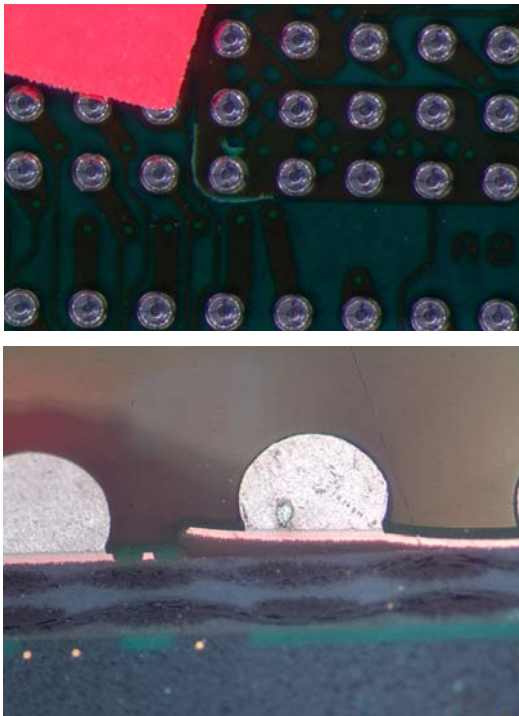


Fig. 12: Photomicrographs showing BGA F473 SN13 solder mask crack (top) and ball side copper plane separation from the BGA substrate interconnect (bottom) found after ball attachment.

Typical photomicrographs of the electroless nickel layer before and after reballing are shown in Fig. 15. As indicated in Table 4, the reduction in average electroless nickel was typically less than a micron after reballing. This minimal level of dissolution is generally consistent with other investigator's findings that negligible ENIG dissolution occurs after tin-lead reballing [12]. At a thickness of 4.34 microns, the X1148 had the thinnest average electroless nickel, while at 8.84 microns the L256 had the thickest nickel layer. The fact that the X1148 sample after reballing had a slightly greater nickel thickness than the as-received sample indicates that there is some part-to-part variation in nickel layer thickness, probably less than a micron.

SAM and Visual Delamination Assessment Results

CSAM measurements and visual inspections at 40x were performed on a minimum of 10 components in the "as-received" condition and same components after reballing. A sample CSAM image and typical inspection summary are provided in Fig. 16. No delamination conditions exceeding our acceptance criteria (defined in the Method section) were found on the M90, L256 or the F473 BGAs. Note that the X1148 could not be imaged because of the presence of a cavity under the lid over the die. The M90 device exhibited one suspect area that was verified by cross-sectioning not to be delamination (see Fig. 17).

Warpage Measurement Results

In general, BGA warpage could impact soldering processes or increase solder stresses during thermal cycling in service. In Fig. 18 through Fig. 21, the warpage results are given for the as-received BGAs and the reballed BGAs.

Three of the BGA types (M90, L256 and F473) exhibited a slight increase in warpage on the reballed samples. The L256 BGA exhibited the greatest increase in warpage (50 microns at 245 °C). An increase in warpage after reballing suggests that the polymer insulating materials have increased in modulus (e.g. increased degree of cure).

The surface contours at 245 °C of the as-received and the reballed L256 BGAs are shown in Fig. 22 and Fig. 23. Examining the warpage of the L256 BGA further, Fig. 24 shows the surface contours at the typical maximum tin-lead soldering temperature of 220 °C. At this temperature, the warpage was 81 microns which compares well with the warpage of the as-received tin-lead version of the L256 shown in Fig. 25.

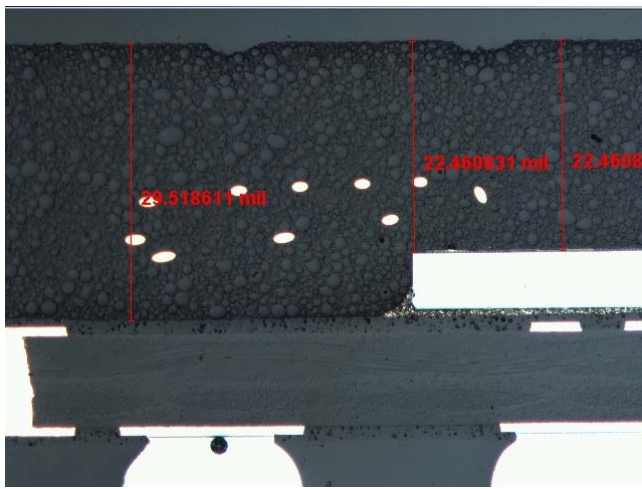


Fig. 13: Typical overall package cross-section (L256 lead-free BGA with the molding compound thicknesses shown)

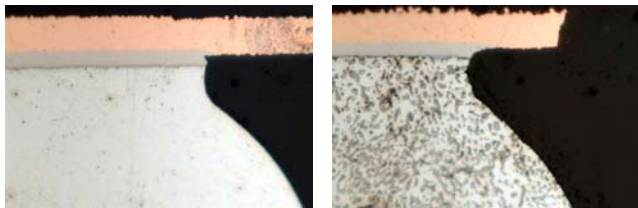


Fig. 14: Typical solder mask defined BGA solder ball and pad BGA solder mask defined pad and ball metallurgy. original lead-free ball (Left) and after reballing (Right). (L256 lead-free BGA shown)

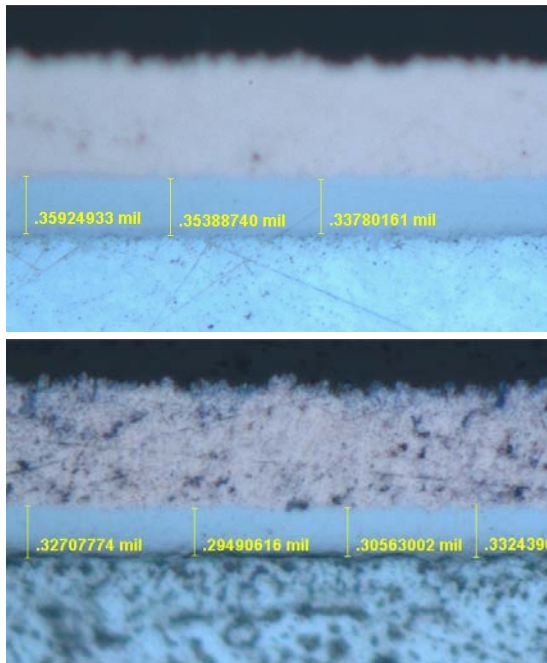


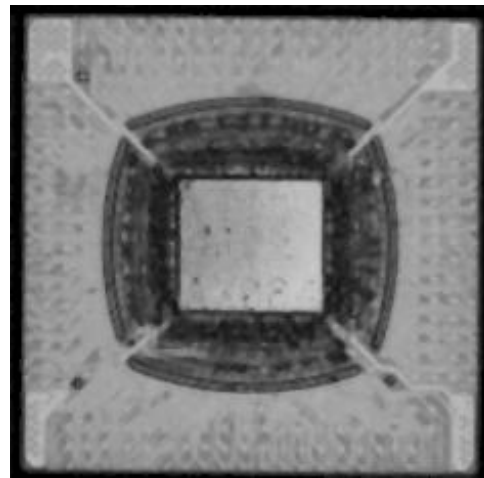
Fig. 15: Typical photomicrographs of the electroless nickel layer thicknesses. As-received part (top) and a part after reballing (bottom). (L256 lead-free BGA shown)

Table 3: BGA Cross-section measurements (microns)

	M90	L256	F473	X1148
Mold thickness adjacent to die	400.1	730.3	831.9	NA
Mold thickness over die	222.3	575.3	501.7	NA
Die thickness	143.5	162.6	279.4	793.8
Die adhesive thickness	31.8	19.1	31.8	76.2
Interconnect substrate thickness	152.4	254	212.1	1073.2
Pad Cu thickness	25.4	25.4	25.4	25.4
SMD pad diameter	393.7	335.3	387.4	406.4
Solder mask thickness	43.2	38.1	39.4	44.5

Table 4: Electroless nickel thickness (microns)

	Avg	Min	Max	Range
As-received				
M90	6.87	6.53	7.21	0.69
L256	8.84	8.56	9.12	0.56
F473	6.67	6.40	6.93	0.53
X1148	4.34	4.06	4.62	0.56
Reballed				
M90	5.72	5.59	5.84	0.25
L256	7.95	7.47	8.43	0.97
F473	5.52	4.78	6.27	1.50
X1148	4.43	4.37	4.50	0.13



BGA Characterization											
Evaluation Criteria (ND = Not Detected)		Sample Identification Number									
		2	5	6	8	9	10	12	13	14	16
External Cracks (Afx Visual)	As Received	ND	ND	ND	ND	ND	ND	ND	ND	ND	ND
	Reballed	ND	ND	ND	ND	ND	ND	ND	ND	ND	ND
Internal Cracks Intersecting Wire Bond	As Received	ND	ND	ND	ND	ND	ND	ND	ND	ND	ND
	Reballed	ND	ND	ND	ND	ND	ND	ND	ND	ND	ND
Delamination % at Die Surface	As Received	ND	ND	ND	ND	ND	ND	ND	ND	ND	ND
	Reballed	ND	ND	ND	ND	ND	ND	ND	ND	ND	ND
Delamination % at Die Paddle	As Received	ND	ND	ND	ND	ND	ND	ND	ND	ND	ND
	Reballed	ND	ND	ND	ND	ND	ND	ND	ND	ND	ND
TE Delamination % at Die attach	As Received	ND	ND	ND	ND	ND	ND	ND	ND	ND	ND
	Reballed	ND	ND	ND	ND	ND	ND	ND	ND	ND	ND

Fig. 16: Typical CSAM image (top) and inspection summary (bottom). (The F473 BGA shown)

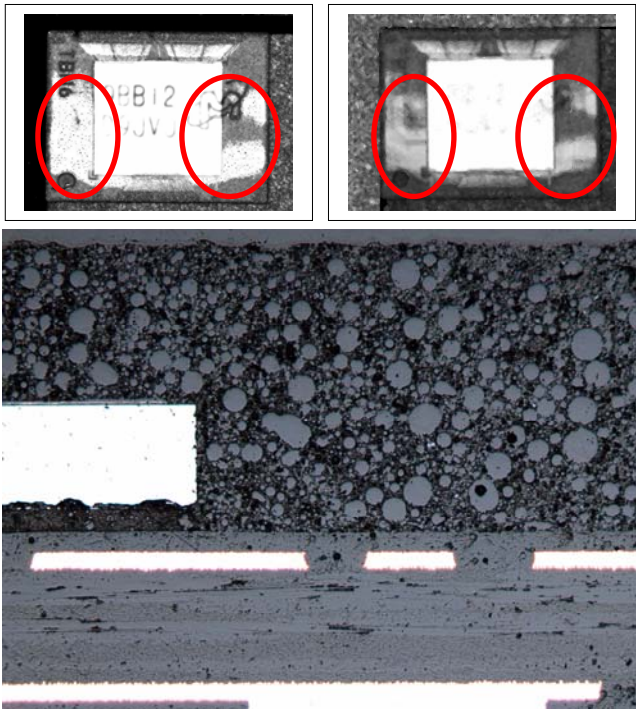


Fig. 17: CSAM and cross-section images of a M90 BGA. The CSAM images of the as-received (top left) and the reballed parts (top right) are shown. The red lines indicated regions of suspected delamination. The cross-section (bottom) shows that no delamination was present.

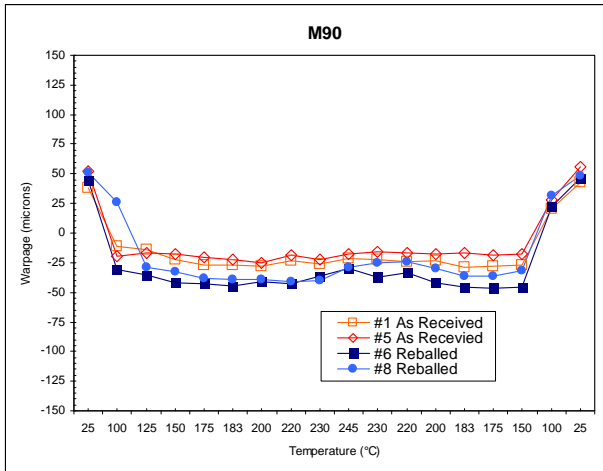


Fig. 18: Warpage on as-received and reballed M90 BGAs

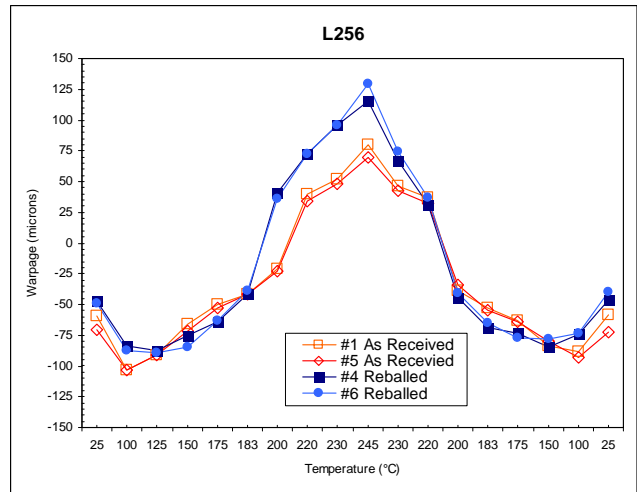


Fig. 19: Warpage on as-received and reballed L256 BGAs

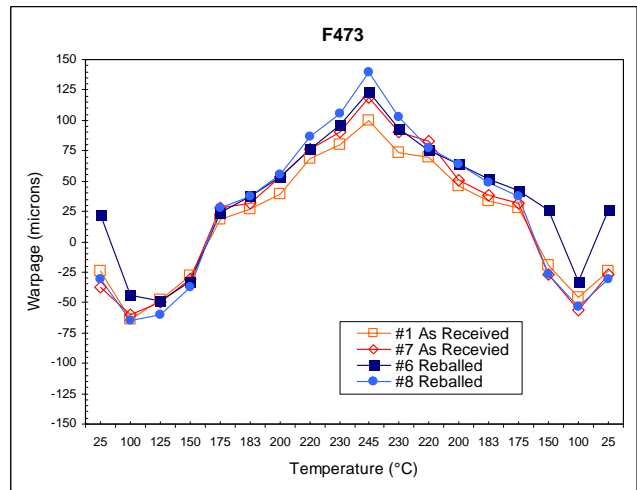


Fig. 20: Warpage on as-received and reballed F473 BGAs

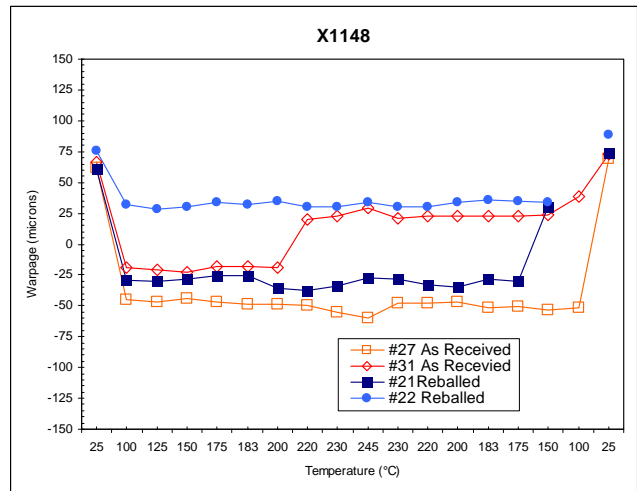


Fig. 21: Warpage on as-received and reballed X1148 BGAs

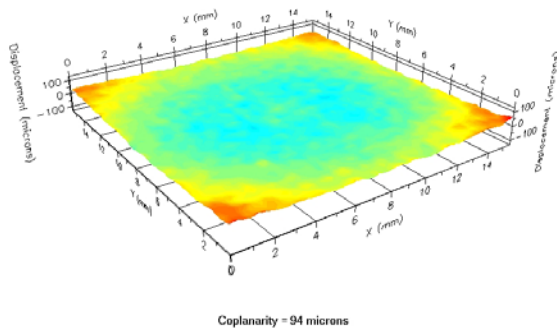


Fig. 22: Warpage of as-received L256 SN1 at 245°C. Coplanarity = 94 microns

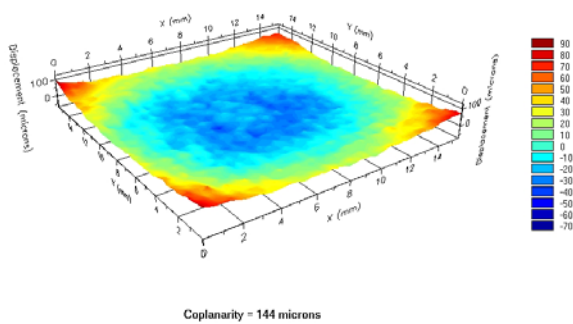


Fig. 23: Warpage of the reballed L256 SN6 at 245°C. Coplanarity = 144 microns.

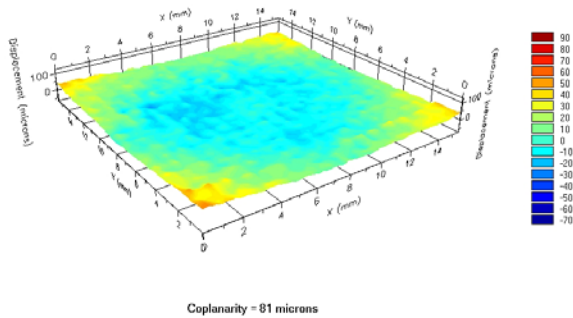


Fig. 24: Warpage of the reballed L256 SN6 at 220 °C. Coplanarity = 81 microns.

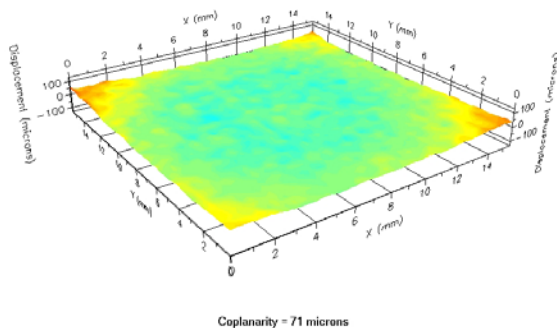
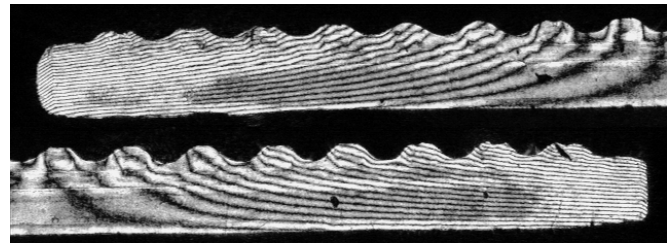


Fig. 25: Warpage of the as-received tin-lead version of the L256 SN5 at 220 °C. Coplanarity = 71 microns.

Warpage values around 75 microns typically have not resulted in soldering issues. The M90 and the F473 BGAs reballed samples exhibited slightly more warpage than the as-received parts. The warpage behavior trends of the X1148 BGA were not clear and may have been complicated by the large metal lid on the device.

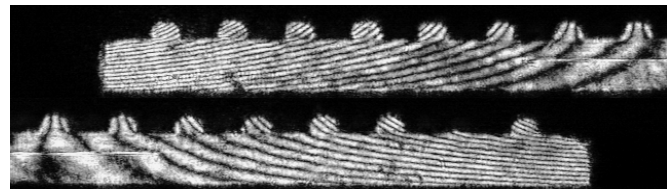
Coefficient of Thermal Expansion Measurement Results

BGAs have two distinct CTE values. One is the CTE under the die region, which is primarily driven by the die, because of its low coefficient of expansion and high modulus. CTE values under the die typically range from 6 to 12-ppm/°C. The other CTE value of concern is the CTE from outer ball to outer ball. Typically, the die dimension is a small portion of the overall size of the BGA and the CTE from ball-to-ball is driven by the BGA interconnect and overmold materials. CTE values from ball-to-ball typically range from 9 to 15-ppm/°C. Some typical Moiré fringe patterns are shown in Fig. 26 and Fig. 27. A summary of the CTE data of as-received and reballed BGAs is shown in Fig. 28. The CTE of the reballed BGAs might be slightly reduced for the M90 BGA as compared to the as-received BGAs. However, the CTEs for the remaining BGAs were similar between the as-received and the reballed BGAs.



Replication Temperature = 80 °C and
 Room Temperature = 22.5 °C then $\Delta T = 57.5$ °C
 Sample Length: 24.02mm and length of die: 5.84mm
 CTE (End to End, Nf = 31) = 9.35ppm/°C
 CTE (Under the die, Nf = 7) = 8.69ppm/°C
 (fringe count was made approximately 0.5 mm below the ball to package interface)

Fig. 26: L256 SN 16 Moiré fringe pattern for an as-received condition BGA



Replication Temperature = 80 °C and
 Room Temperature = 20.7 °C then $\Delta T = 59.3$ °C
 Sample Length: 24mm and Die Length: 5.77mm
 CTE (End to End, Nf = 33) = 9.66ppm/°C
 CTE (Under the die, Nf = 6) = 7.31ppm/°C

Fig. 27: L256 SN 6 Moiré fringe pattern for a reballed BGA

BGA Ball Shear and Ball Pull Measurement Results

Solder ball pull and shear testing gives an indication of the interconnect strength and failure mode under various rates of loading. The goal of this testing was to determine the robustness of the solder ball interface with the attachment pad, and observe any changes as a function of the reballing process. BGAs typically have three failure modes.

- Bulk solder failure
 - Failures in the bulk solder are ductile failures typically observed in tin-lead assemblies or lead-free assemblies at low loading velocities.
- Intermetallic layer failure
 - Failures indicate a weak intermetallic layer or can be due to the increased stiffness in the lead-free solder balls.
- Pad cratering failure
 - Failure represents a strong intermetallic layer and more brittle PWB dielectrics. Typically observed in lead-free assemblies.
- Extrusion failure
 - Occurs when the solder pulls out of the instrument ball pull gripping tool.
- Mixed mode failure
 - Failure that exhibits a combination of intermetallic and bulk solder failure that represents a pad that has some weaker intermetallic regions.

High speed testing caused some brittle intermetallic and pad cratering failures in the lead-free balls. The results for the high speed ball pull and shear tests are shown in Fig. 29 through Fig. 36. The tests on the reballed tin-lead components produced almost exclusively ductile failures (i.e. failure in the bulk solder), indicating a good bond between the solder and the metal pad to which it was attached, and a good bond between the pad and the BGA interconnect. The “as-received” lead-free BGAs exhibited higher pull and shear forces as well as more instances of brittle (interfacial) failures than the reballed tin-lead components. This result was expected because lead-free solders are stronger and stiffer than tin-lead solder, as observed by other investigators [7].

Both the L256 and the X1148 devices had samples that were tin-lead in as-received condition, which allowed for a direct comparison to the reballed devices. The results indicate that at worst, the reballed devices have the same strength, and at best, the reballed devices are 10% stronger than the as-received tin-lead devices. The results provide confidence that the reballing process results in sufficiently well attached balls. In addition, since no intermetallic failures or pad cratering failures were observed, the reballing process yielded sufficient interfacial strength.

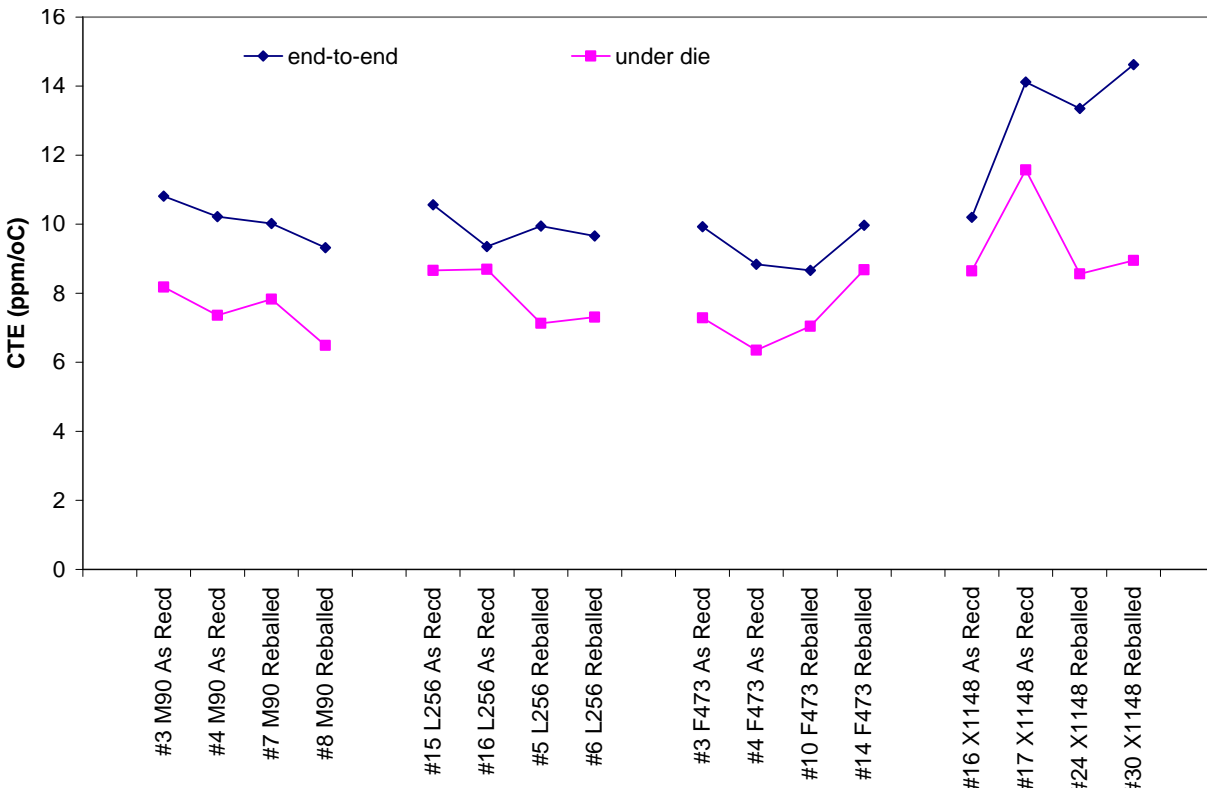


Fig. 28: Summary of BGA CTE data of as-received and reballed BGAs

M90 - Ball Shear			
As-Received Pb-Free			
	Force (grams)	Energy (mJ)	Failure Modes
Average	1444.9	2.1	4 Bulk Solders
Minimum	1118.4	0.7	9 Interfacial
Maximum	1722.7	3.9	0 Pad
Range	604.3	3.2	0 Extrusions
Std. Dev.	173.9	1.1	5 Mixed
Post-Reballing SnPb			
	Force (grams)	Energy (mJ)	Failure Modes
Average	1129.8	2.4	18 Bulk Solders
Minimum	1041.5	1.9	0 Interfacial
Maximum	1244.7	3.0	0 Pad
Range	203.2	1.1	0 Extrusions
Std. Dev.	55.1	0.3	0 Mixed

Fig. 29: M90 Ball shear results for as-received and reballed BGAs

L256 - Ball Shear			
As-Received SnPb			
	Force (grams)	Energy (mJ)	Failure Mode
Average	1076.7	2.2	24 Bulk Solders
Minimum	937.4	1.7	0 Interfacial
Maximum	1175.2	3.5	0 Pad
Range	237.8	1.8	0 Extrusions
Std. Dev.	45.1	0.4	0 Mixed
As-Received Pb-Free			
	Force (grams)	Energy (mJ)	Failure Mode
Average	1777.0	4.1	15 Bulk Solders
Minimum	1360.2	1.8	1 Interfacial
Maximum	2203.6	5.6	0 Pad
Range	843.4	3.9	0 Extrusions
Std. Dev.	210.1	0.9	8 Mixed
Post-Reballing SnPb			
	Force (grams)	Energy (mJ)	Failure Mode
Average	1221.8	2.4	24 Bulk Solders
Minimum	1107.4	2.1	0 Interfacial
Maximum	1328.3	3.3	0 Pad
Range	220.9	1.2	0 Extrusions
Std. Dev.	46.3	0.3	0 Mixed

Fig. 30: L256 Ball shear results for as-received and reballed BGAs

F473 - Ball Shear			
As-Received Pb-Free			
	Force (grams)	Energy (mJ)	Failure Mode
Average	1650.6	4.3	26 Bulk Solders
Minimum	1441.6	3.1	0 Interfacial
Maximum	1872.1	13.2	0 Pad
Range	430.5	10.1	0 Extrusion
Std. Dev.	99.6	1.7	5 Mixed
Post-Reballing SnPb			
	Force (grams)	Energy (mJ)	Failure Mode
Average	1203.5	2.5	32 Bulk Solders
Minimum	1048.7	2.1	0 Interfacial
Maximum	1292.4	2.8	0 Pad
Range	243.7	0.7	0 Extrusions
Std. Dev.	60.3	0.2	0 Mixed

Fig. 31: F473 Ball shear results for as-received and reballed BGAs

X1148 - Ball Pull			
As-Received SnPb			
	Force (grams)	Energy (mJ)	Failure Modes
Average	2076.2	5.5	31 Bulk Solders
Minimum	1956.6	4.3	0 Interfacial
Maximum	2211.8	7.8	0 Pad
Range	255.2	3.5	1 Extrusions
Std. Dev.	67.9	0.7	0 Mixed
Post-Reballing SnPb			
	Force (grams)	Energy (mJ)	Failure Modes
Average	2204.3	8.1	27 Bulk Solders
Minimum	2077.0	4.8	0 Interfacial
Maximum	2328.3	10.8	0 Pad
Range	251.3	6.0	5 Extrusions
Std. Dev.	63.9	1.5	0 Mixed

Fig. 32: X1148 Ball pull results for as-received and reballed BGAs

M90 - Ball Pull			
As-Received Pb-Free			
	Force (grams)	Energy (mJ)	Failure Modes
Average	1202.2	2.3	20 Bulk Solders
Minimum	1063.3	1.2	5 Interfacial
Maximum	1274.0	3.5	0 Pad
Range	210.7	2.3	5 Extrusions
Std. Dev.	54.0	0.5	1 Mixed
Post-Reballing SnPb			
	Force (grams)	Energy (mJ)	Failure Modes
Average	999.0	2.1	29 Bulk Solders
Minimum	942.2	1.7	0 Interfacial
Maximum	1057.5	3.0	0 Pad
Range	115.3	1.3	2 Extrusions
Std. Dev.	32.6	0.3	0 Mixed

Fig. 33: M90 Ball pull results for as-received and reballed BGAs

L256 - Ball Pull			
As-Received SnPb			
	Force (grams)	Energy (mJ)	Failure Mode
Average	1283.7	2.1	18 Bulk Solders
Minimum	1109.0	1.3	11 Interfacial
Maximum	1405.7	4.0	0 Pad
Range	296.7	2.6	0 Extrusions
Std. Dev.	77.2	0.6	3 Mixed
As-Received Pb-Free			
	Force (grams)	Energy (mJ)	Failure Mode
Average	1903.9	3.5	18 Bulk Solders
Minimum	1587.2	0.7	11 Interfacial
Maximum	2125.1	6.4	1 Pad
Range	537.9	5.6	2 Extrusions
Std. Dev.	113.9	1.3	0 Mixed
Post-Reballing SnPb			
	Force (grams)	Energy (mJ)	Failure Mode
Average	1535.8	2.8	31 Bulk Solders
Minimum	1423.0	2.2	0 Interfacial
Maximum	1641.5	6.1	0 Pad
Range	218.5	3.9	0 Extrusions
Std. Dev.	55.7	0.7	1 Mixed

Fig. 34: L256 Ball pull results for as-received and reballed BGAs

F473 - Ball Pull			
As-Received Pb-Free			
	Force (grams)	Energy (mJ)	Failure Mode
Average	1193.3	1.4	16 Bulk Solders
Minimum	1063.0	0.6	0 Interfacial
Maximum	1256.0	3.0	14 Pad
Range	193.0	2.4	1 Extrusion
Std. Dev.	39.8	0.6	0 Mixed
Post-Reballing SnPb			
	Force (grams)	Energy (mJ)	Failure Mode
Average	1038.6	1.6	26 Bulk Solders
Minimum	870.5	0.9	0 Interfacial
Maximum	1181.2	2.7	0 Pad
Range	310.7	1.7	6 Extrusions
Std. Dev.	55.9	0.5	0 Mixed

Fig. 35: F473 Ball pull results for as-received and reballed BGAs

X1148 - Ball Shear			
As-Received SnPb			
	Force (grams)	Energy (mJ)	Failure Modes
Average	1825.3	4.0	30 Bulk Solders
Minimum	1664.1	3.2	0 Interfacial
Maximum	1929.0	5.0	0 Pad
Range	264.9	1.8	0 Extrusions
Std. Dev.	73.0	0.5	0 Mixed
Post-Reballing SnPb			
	Force (grams)	Energy (mJ)	Failure Modes
Average	1888.7	5.1	32 Bulk Solders
Minimum	1719.3	3.7	0 Interfacial
Maximum	2099.4	6.7	0 Pad
Range	380.1	3.0	0 Extrusions
Std. Dev.	82.8	0.6	0 Mixed

Fig. 36: X1148 Ball shear results for as-received and reballed BGAs

BGA Analytical Modeling Results

The transient thermal modeling results for the L256 correlated well with the measured temperatures during ball removal as was previously illustrated by the bold lines in Fig. 10. The maximum temperature of the die (top center) was 216.5 °C during ball removal.

Next the static warpages of the BGAs were evaluated. The BGA modeling material properties were selected to match the static warpage measurements. Fig. 37 shows that the analytical prediction for overall warpage correlated well to the measured data for the L256 and the F473 BGAs.

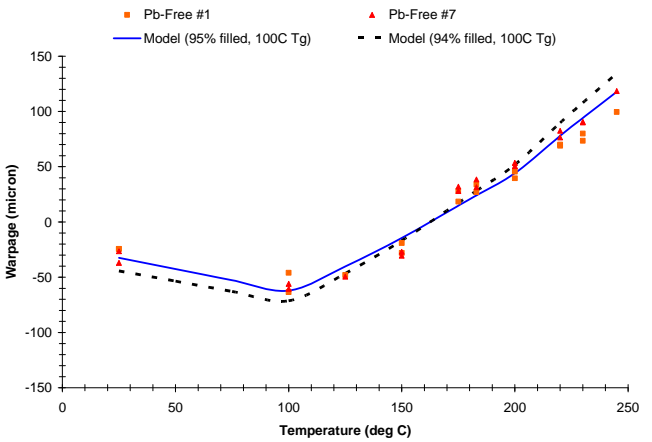
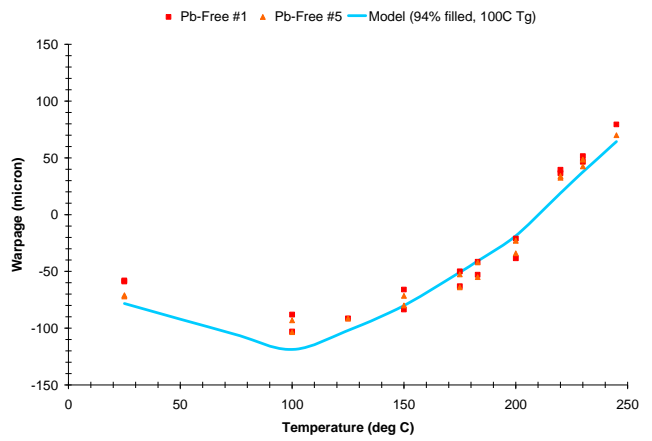


Fig. 37: Comparison between computed and measured warpage. for the L256 (A) and F473 (bottom). Square and round symbols represent two individual sets of measured warpage data for each BGA type.

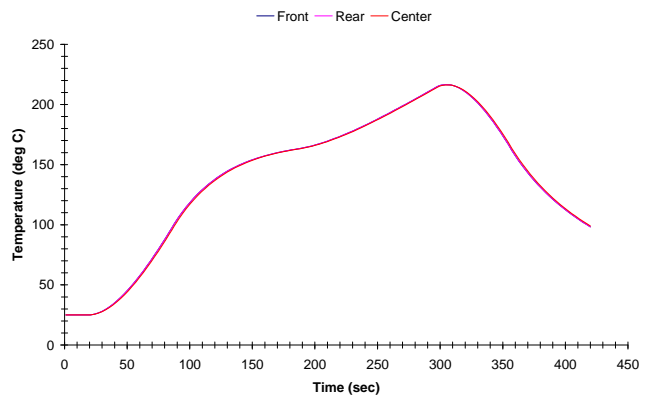


Fig. 38: Thermal analysis results of the package temperature during a typical surface mount reflow soldering process. Temperatures for the front of the package, the top center of the die and the rear of the package were computed to be nearly the same.

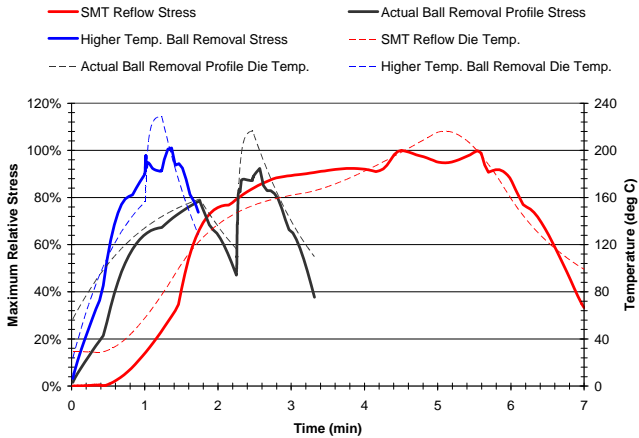


Fig. 39: Comparison of maximum relative package stresses for three different thermal profiles. The stresses are normalized to the maximum stress observed during surface mount reflow soldering.

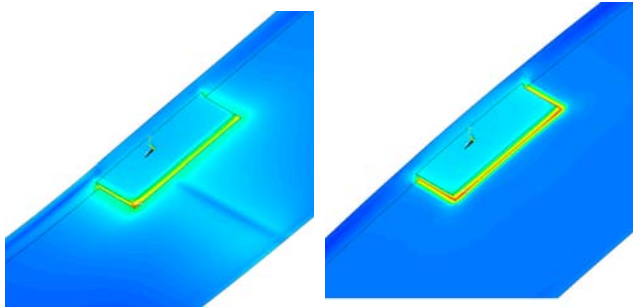


Fig. 40: Stress plot of L256 BGA during ball removal thermal exposure. The left image shows the solder wave front when it is mid way in its traverse across the package at 2.26 minutes (135.59 seconds). The right image show the stress plot when the maximum stress occurs at 2.57 minutes (154.26 seconds). The highest stresses are red shades and low stresses are blue shades.

The model was then used to compare the stresses in the BGA during the ball removal. The stresses are normalized to the maximum stress that would normally be observed during surface mount reflow (stresses equal to the SMT reflow stress are plotted as a magnitude of 100%). The surface mount reflow thermal profile has a maximum temperature of 216.3 °C at the die (top center), shown for reference in Fig. 38. In contrast to the actual ball removal process (Fig. 10), there is minimal temperature variation across the package during the SMT reflow profile. The stresses computed during reballing are compared to the SMT reflow stresses in Fig. 39. In addition, to assess the actual ball removal profile, the stress for a ball removal profile with a higher preheat temperature and a higher die temperature was evaluated. The computed maximum stress during the actual ball removal thermal profile was less than the surface mount solder reflow. The maximum stress was located around the corners of the die as shown in Fig. 40. The higher temperature ball removal profile resulted in the largest stresses.

The model reveals that there is interaction between the rate of temperature change and the maximum temperature that influences the maximum package stress. As highlighted in Table 5, there are two instances where high stress occurs near the peak temperature. Furthermore, the higher the package temperature, the higher the maximum stress. This suggests that both the temperature gradient and the die (top center) temperature contribute to the stress state. A detailed study of this behavior is the topic of future work.

Table 5: Summary of computed peak temperatures and relative stresses

	Time (sec)	Time from Tmax	Die Temp. (°C)	Relative Mold Stress
SMT Reflow	270.4	-36.2	198.5	100.0%
	306.6	0.0	216.3(max)	94.7%
	332.6	26.0	199.5	99.9%
Actual ball removal	141.3	-6.9	208.8	87.8%
	148.2	0.0	216.5(max)	87.3%
	154.3	6.0	199.4	92.3%
Higher temp. ball removal	60.9	-12.4	168.1	97.7%
	73.3	0.0	228.9(max)	91.3%
	82.0	8.7	195.6	101.0%

Thermal Cycling Results

The M90, L256 and F473 test module assemblies are currently being thermal cycled. The thermal cycling results are summarized in Table 6. Each board has 12 BGAs that are continuously electrically monitored using boundary scan circuitry. The F473 module does not have operational monitoring circuitry and was cross-sectioned at 136 cycles to assess the integrity of the solder joints. No assembly solder fractures or other anomalies were observed (See Fig. 41). Other investigators have observed good assembly thermal cycling performance of reballed BGAs after 1000 cycles (-25° C/+125 °C, 15 minute ramps and dwells), as well as vibration and shock [14].

Table 6: Thermal cycling results (-55 to +95 °C ½ hour ramps and dwells)

BGA Type	Module Serial Number	Number of Cycles	Comments
M90	M1	675	No electrical failures and cycling continuing
L256	L1	281	No electrical failures and cycling continuing
F473	F1	136	Non-monitored: Cross-sectioning complete
F473	F2	663	Non-monitored: Cross-sections planned at 1000 cycles

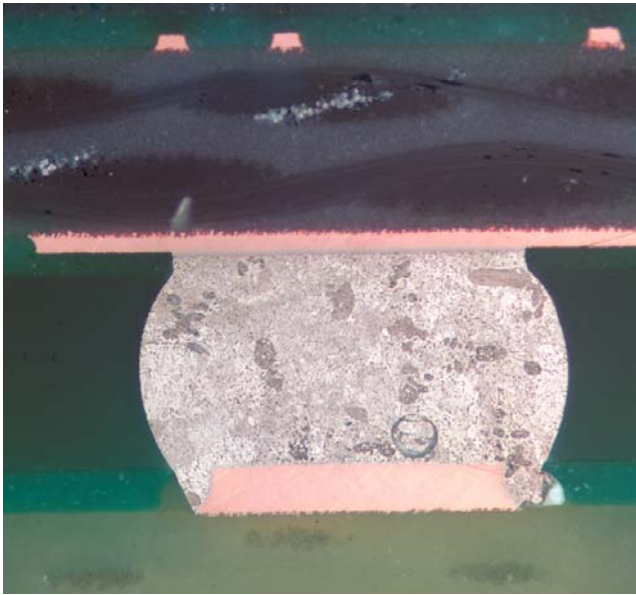


Fig. 41: Typical cross-section of F473 after 136 thermal cycles from -55 to +95 °C.

SUMMARY

With careful attention to detail, BGA reballing remains a viable solution to manage the obsolescence of tin-lead ball metallurgy. The cross-section evaluation provided the key package construction details needed for modeling. The scanning acoustic microscopic examination was generally successful in assuring that the package structures did not delaminate during the reballing process, though it was not useful for the package with the lid. Visual inspection of the package is an important part of the reballing quality verification. Warpage measurement appears to be more useful than coefficient of thermal expansion measurement in assessing BGA changes during reballing. However, warpage change acceptance limits are still need. The increase in warpage observed after reballing suggests that the polymer insulating materials may have increased in modulus (e.g. increased degree of cure). The ball shear and ball pull tests verified that the pad-to-package interconnections were not compromised by reballing. The thermomechanical stress modeling effort needed the cross-sectioning, warpage and CTE measurements. In general, these preliminary modeling efforts suggest that increasing maximum temperature of the die (top center) during ball removal increases the maximum stresses within the part and that the location of the maximum stress is near the die corners and edges. It is hopeful that efforts such as this will contribute to the body of knowledge needed for industry standard development [15].

FUTURE WORK

Assembly thermal cycling is continuing and assembly vibration and mechanical shock testing are planned. The X1148 BGA module assemblies will be completed and subjected to thermal cycling, vibration and mechanical shock. Further modeling work will be pursued to assess process sensitivity of ball removal variables (e.g. preheat temperatures, ball removal temperatures or ball attach

temperatures). In addition, the modeling effort will be extended to develop a basis for similarity assessments among different BGA packages intended for reballing.

ACKNOWLEDGEMENTS

Thanks to Jim Carrigan, David Grant, and Hal Rotchadl of Premier Semiconductor Inc. for reballing services, visual inspection and thermal characterization and to Wayne Jones and Brian Roggeman at Universal Instruments Corp., in Conklin, NY, for the BGA characterization service. In addition, the authors would like to thank Dr. Park at the Binghamton University Mechanical Engineering Optomechanics Laboratory in Binghamton, NY for his help with the CTE measurements. The authors also wish to thank Dr. Sam Saha, Ted Hartford and Joe Kane from BAE Systems in Johnson City for their assistance on this project.

REFERENCES

- [1] European Union (February 13, 2003). Directive 2002/95/EC/ of the European Parliament and of the Council of 27 January 2003 on the restriction of the use of certain hazardous substances in electrical and electronic equipment. Official Journal of the European Union.
- [2] Ganesan S, Pecht M. Lead-free Electronics, John Wiley & Sons, Inc. NY, USA, 2006.
- [3] "The Lead Free Electronics Manhattan Project - Phase I Report," Completed under U.S. Government Contract No. N00014-08-D-0758, The Benchmarking and Best Practices Center of Excellence at ACI Technologies, Inc., Philadelphia, PA, July, 30 2009
http://www.navyb2pcoe.org/b2p_news.html and
<https://acc.dau.mil/leadfree>
- [4] GEIA-HB-0005-2, Technical Guidelines for Aerospace and High Performance Electronic Systems Containing Pb-free Solder and Finishes, Tech America Inc., Arlington, VA USA (formerly Government Electronic Industries Association)
- [5] Woodrow T.A., JCAA/JG-PP Lead-Free Solder Project: -55 to +125 ° C Thermal Shock Test; March 1, 2006. Also published in The Proceedings of SMTA International Conference, Rosemont, IL, September 24-28, 2006.
- [6] Woodrow T.A., The Effects of Trace Amounts of Lead on the Reliability of Six Lead-Free Solders, Proceedings of the 3rd International Conference on Lead-Free Components and Assemblies, San Jose, CA April 23-24, 2003.
- [7] Nie L, Osterman M, Pecht M, Song F, Lo J, Lee S W, Solder Ball Attachment Assessment of Reballled Plastic Ball Grid Array Packages, IEEE Trans. Components. and Packaging Tech., Vol. 32, No. 4, December 2009, pp. 901-908

- [8] Cirimele R, BGA Reballing Reliability: A Study of Multiple Reball Processes Looks at Copper Dissolution and Functionality, Circuits Assembly, June 2009, pp. 27-29.
- [9] Muonio J, and Stadem R, Solder Ball Attachment Using Laser Soldering, Circuits Assembly, October 2008.
- [10] Winslow R, BGA Reballing Overview, Presentation at the Aerospace Industries Association – Lead-free Electronics in Aerospace Project (AIA-LEAP) working group meeting , June 3, 2007.
- [11] Han B and Guo Y, Determination of an Effective Coefficient of Thermal Expansion of Electronic Packaging Components: A Whole-Field Approach, IEEE Trans. on Components, Packaging and Manufacturing Technology-Part A, Vol. 19, No. 2, June 1996, pp 240 - 247
- [12] Cruz MM, and Winslow R, Interfacial Reactions between Sn63-Pb37 Solder and Electroless/Electrolytic Nickel UBM, University of Maryland CALCE Tin Whisker and Lead-free Rework Workshop, College Park Maryland, November 2008.
- [13] Meschter S, Mckeown S, Effect of Hot Solder Dipping on Part Stresses, Proceedings of IMECE2008, 2008 ASME International Mechanical Engineering Congress and Exposition, October 31-November 6, 2008, Boston MA.
- [14] Davisson M, An OEM Perspective on Re-balling and case history, University of Maryland CALCE Tin Whisker and Lead-free Rework Workshop, College Park Maryland, November 2008.
- [15] GEIA-STD-0015, Requirements for BGA Reballing in Aerospace and High Performance Electronics, Draft Document, Tech America Inc., Arlington, VA USA (formerly Government Electronic Industries Association)